

王楠, 王帅, 徐俊平, 等. 添加金属(氢)氧化物对木质素腐殖化作用的影响机理[J]. 农业环境科学学报, 2019, 38(11): 2528–2535.

WANG Nan, WANG Shuai, XU Jun-ping, et al. Mechanism behind the influence of metal (hydr) oxides on humification of lignin[J]. Journal of Agro-Environment Science, 2019, 38(11): 2528–2535.

添加金属(氢)氧化物对木质素腐殖化作用的影响机理

王楠¹, 王帅¹, 徐俊平¹, 王语¹, 窦森^{2*}

(1. 吉林农业科技学院农学院, 吉林 吉林 132101; 2. 吉林农业大学资源与环境学院, 长春 130118)

摘要:为研究金属(氢)氧化物在木质素腐殖化作用中的催化作用,采用液体摇瓶培养法,在木质素培养液中添加针铁矿、三羟铝石和 $\delta\text{-MnO}_2$,接种混合菌株悬液后启动110 d的培养试验,动态收集沉淀物质并用 H_2O_2 去除氧化物表面的有机成分,应用SEM、FTIR和XRD技术对其结构特征进行分析。结果表明:针铁矿参与木质素腐殖化作用后,小颗粒比例增加且边缘棱角锐化,表面水合羟基与微生物及其转化的木质素间形成氢键,使表面水合羟基($-\text{OH}_2^+$)及结晶水O-H的缔合程度增强。Fe-OH的质子化使Fe-O的振动频率增强,配体交换和氢键作用是针铁矿催化木质素腐殖化作用的主要机制;三羟铝石参与木质素腐殖化作用后,晶粒轮廓更加清晰,粒径减小且有聚集趋势,表面Al-OH以氢键形式与微生物及其转化的木质素结合,增加了水合基振动频率,部分OH基团还可被微生物及其转化木质素的羧基取代,弱化了 AlO_4 四面体和 AlO_6 八面体上的Al-O键,水桥键及螯合物的形成使Al-OH $_2^+$ 的振动频率增强;疏水作用是 $\delta\text{-MnO}_2$ 参与木质素转化的主要机制,反应后颗粒结合更加松散,微纳米球边缘锐化,表面结晶水脱除,Mn-OH的去质子化使O-Mn-O的振动频率增加。研究表明,上述3种金属(氢)氧化物均是通过表面羟基与金属含氧基团来催化木质素的腐殖化作用,而其本身并未发生物理相改变。

关键词:针铁矿;三羟铝石; $\delta\text{-MnO}_2$;木质素;腐殖化作用

中图分类号:X132 文献标志码:A 文章编号:1672-2043(2019)11-2528-08 doi:10.11654/jaes.2019-0717

Mechanism behind the influence of metal(hydr) oxides on humification of lignin

WANG Nan¹, WANG Shuai¹, XU Jun-ping¹, WANG Yu¹, DOU Sen^{2*}

(1. College of Agriculture, Jilin Agricultural Science and Technology University, Jilin 132101, China; 2. College of Resources and Environmental Sciences, Jilin Agricultural University, Changchun 130118, China)

Abstract: Metal(hydr) oxides have a catalytic role in lignin humification, and the related abiotic mechanisms remain to be revealed. The method of liquid shake flask culture was adopted; during the process, goethite, bayerite and $\delta\text{-MnO}_2$ were added to the fluid medium containing lignin, and then a microbial suspension was inoculated for the culture period of 110 d. Precipitates were collected dynamically, and the organic components attached on the metal(hydr) oxides were removed using H_2O_2 solution and their structural characteristics were analyzed by scanning electron microscopy(SEM), Fourier transform infrared spectroscopy(FTIR), and X-ray diffraction analysis(X-ray diffraction, XRD). The results showed that the proportion of small particles was increased, and their edges were sharpened after the participation of goethite in lignin humification. Hydrated hydroxyl groups on the surface of goethite could form H-bonds with the inoculated strains and their transformed lignin, enhancing the degree of association between surface hydrated hydroxyl groups ($-\text{OH}_2^+$) and O-H of crystal H_2O . Protonation of Fe-OH enhanced the vibration frequency of Fe-O. Ligand exchange reactions and H-bonds were the main mechanisms by which goethite catalyzed the humification of lignin; After participating in lignin humification, crystal particles of bayerite had a clearer profile, and particles of smaller size had a tendency to aggregate. Al-OH on the surface of bayerite could combine with the inoculat-

收稿日期:2019-06-28 录用日期:2019-09-02

作者简介:王楠(1982—),女,吉林九台人,博士,副教授,从事土壤肥力调控研究。E-mail:wangnan664806@126.com

*通信作者:窦森 E-mail:dousen1959@126.com

基金项目:国家重点研发计划项目(2018YFD0300207-1);国家自然科学基金项目(41401251, 41571231);吉林农业科技学院种子基金项目(吉农院合字[2018]第7004号)

Project supported: The National Key Research and Development Program of China(2018YFD0300207-1); National Natural Science Foundation of China (41401251, 41571231); The Seed Fund Project of Jilin Agricultural Science and Technology University(20187004)

ed strains and their transformed lignin through H-bonds to enhance the vibration frequency of hydrated hydroxyl groups; simultaneously, a part of OH groups of bayerite could also be replaced by the carboxyl groups from microbial strains and their transformed lignin, which could weaken Al-O bonds in AlO_4 tetrahedron and AlO_6 octahedron. The vibration frequency of $\text{Al}-\text{OH}_2^+$ was enhanced by the water bridges and the formation of a chelate complex. Hydrophobic interaction was the main mechanism of $\delta-\text{MnO}_2$ involvement in lignin transformation. After the transformation, the particle binding strength of $\delta-\text{MnO}_2$ tended to weaken, edges of micro-nanospheres were sharpened, and surface crystal H_2O tended to get removed. Protonation of $\text{Mn}-\text{OH}$ increased the vibration frequency of $\text{O}-\text{Mn}-\text{O}$. All the above three metal (hydr) oxides catalyze the humification of lignin by the action of surface hydroxyl groups and metal oxygen-containing groups, without themselves undergoing any phase change.

Keywords: goethite; bayerite; $\delta-\text{MnO}_2$; lignin; humification

作为自然界中含量仅次于纤维素且有着三维结构的高分子聚合物,木质素占生物质木质纤维成分的10%~30%^[1],是植物骨架结构的重要组分,因其结构复杂、不易分解,在植物细胞壁中缠绕纤维素和半纤维素而生,所以对两者具有抵御微生物分解的保护作用^[2]。而在堆肥过程中,木质素难降解的特性就成为堆肥腐解进程的限速因子。

土壤腐殖质(HS)形成与木质素降解关系密切^[3],而微生物又是影响HS形成的直接驱动因素^[4],由此可作出假设:微生物+木质素=HS。然而,在远古时代,地球陆地表面由各类岩石组成,HS的最初形成无法摆脱矿物的参与,在此过程,矿物与微生物间的交互作用是塑造岩石圈、形成土壤的关键^[5],即“微生物+木质素+矿物=HS”的科学假设更符合客观规律。作为土壤学世界领域的科学难题,HS分子结构异质性不仅决定于有机碳源性质、微生物群落结构,而且还与环境介质有关,而矿物组成作为最重要的环境介质,其所发挥的非生物作用在HS形成中不可或缺。化学催化聚合学说认为,木质素的分解产物,如酚、醌和脂类化合物能够在黏土矿物表面吸附的Fe、Al氧化物的催化下与氨基酸聚合形成HS^[6]。Tan^[7]指出,梭菌、芽孢杆菌和放线菌等有益微生物菌群能够在堆肥加热和嗜热阶段分解和转化有机物质,产生HS的前体物质并最终聚合形成HS,在此过程,矿物能够催化氨基酸、糖和酚等前体物质间的缩聚反应^[8]。Fe或Al的(氢)氧化物是土壤正电荷的主要贡献者,土壤有机碳(SOC)的积累和稳定在很大程度上决定于Fe或Al(氢)氧化物对水溶性有机物(DOM)的吸附^[9]。有报道指出^[10],土壤有机质(SOM)含量通常与Fe、Al(氢)氧化物含量成正比。针铁矿能够吸附并稳定有机物质、抑制微生物的分解^[11]。在北极土壤中,氧化还原界面富集的铁能够通过吸附DOM、与颗粒状有机物聚集、不溶性Fe(II)与Fe(III)-有机复合物的凝聚等

多种机制阻碍有机物质的降解^[12]。无定形氢氧化铝能够较强烈地吸附DOM,并通过保护机制使DOM免受土壤微生物的分解^[13]。Miltner等^[14]研究指出,Fe或Al(氢)氧化物能够通过吸附木质素或其氧化的副产物抑制木质素的分解。此外,锰氧化物也是土壤氧化还原过程的主要参与者,对土壤生态系统中HS-酶复合物的形成有促进作用^[15],尤其在Maillard反应中, $\delta-\text{MnO}_2$ 更是充当氧化剂来促进暗色物质的形成。在Fe、Al、Mn氧化物催化加速腐殖化进程方面,人工合成的Mn(IV)-氧化物>Fe(III)-氧化物>Al-氧化物>Si-氧化物^[16],而在提高总腐殖质聚合物产量方面^[17-18],Fe(III)-氧化物>Mn(IV)-氧化物>Al-氧化物>Si-氧化物>无催化剂。Wu等^[19]研究认为,在玉米秸秆堆肥中,MnO₂的添加可在5 d内迅速降低还原糖的浓度并相应提高HS的含量。Yuan等^[20]研究表明,堆肥中Fe(III)氧化物的减少可相应提高胡敏酸中可提取醌类和芳香碳的含量。

综上,以往研究多关注添加氧化物后HS组分及结构特性的变化,以此来探究氧化物的催化作用,对于相关机理的阐述稍显不足。鉴于此,本研究采用液体摇瓶培养法,以木质素为碳源,通过混合菌株悬液的接种,针铁矿、三羟铝石及 $\delta-\text{MnO}_2$ 的添加,对培养110 d期间收集的含有氧化物的沉淀物质,用H₂O₂淋洗去除有机分子,应用SEM、FTIR和X射线衍射技术,以Fe、Al、Mn的(氢)氧化物为第一视角,分析结构特征变化,以此揭示其在HS形成过程中的非生物催化机理。

1 材料与方法

1.1 试验材料

木质素(CAS No [9005-53-2])购于东京化成工业株式会社;针铁矿、三羟铝石和 $\delta-\text{MnO}_2$ 制备方法如下^[11]:针铁矿,称取 $\text{Fe}(\text{NO}_3)_3 \cdot 9\text{H}_2\text{O}$ 50 g于广口塑料瓶

中,加入825 mL蒸馏水使之溶解,在不断搅拌下缓慢滴加2.5 mol·L⁻¹ NaOH溶液至悬液pH 11.9,60 ℃陈化48 h;δ-MnO₂,取180 g MnSO₄·H₂O溶解到1500 mL 29 mmol·L⁻¹的H₂SO₄溶液中,另取120 g KMnO₄溶于1500 mL蒸馏水中,边搅拌边将该溶液缓慢加入到MnSO₄溶液中;三羟铝石,将0.18 mol·L⁻¹的KOH溶液以3 mL·min⁻¹的速度滴加到0.06 mol·L⁻¹ Al(NO₃)₃溶液中,并不断搅拌,直到悬液pH 9.0,室温下老化30 d。上述氧化物经去离子水多次洗涤至洗液近中性,经半透膜渗析后于60 ℃下烘干并磨细过0.25 mm筛,备用。

复合菌株由4种细菌[枯草芽孢杆菌(*B. subtilis*)、巨大芽孢杆菌(*B. megaterium*)、短小芽孢杆菌(*B. pumilus*)和地衣芽孢杆菌(*B. licheniformis*)]、2种放线菌[灰色链霉菌(*S. griseus*)和细黄链霉菌(*S. microflavus*)]和3种真菌[绿色木霉(*T. viride*)、黑曲霉(*A. niger*)和桔青霉(*P. citrinum*)]组成,将9种单一菌株悬液等体积掺混制成复合菌株悬液,悬液中各菌落数如下:*B. subtilis*、*B. megaterium*、*B. pumilus*、*B. licheniformis*、*S. griseus*和*S. citrinum*分别为5.9×10⁶、2.6×10⁶、7.2×10⁶、4.4×10⁶、6.0×10⁹ cfu·mL⁻¹和4.2×10⁹ cfu·mL⁻¹,*T. viride*、*A. niger*和*P. citrinum*孢子数分别为201、68 cfu·mL⁻¹和158 cfu·mL⁻¹。

1.2 试验设计

采用液体摇瓶培养法,培养液配方参照察氏培养基进行,由木质素提供碳源,具体配方如下:NaNO₃ 2.0 g、K₂HPO₄ 1.0 g、KCl 0.5 g、MgSO₄ 0.5 g、FeSO₄ 0.01 g、木质素1.0 g、水1000 mL,无需调节pH。

为了探索Fe、Al、Mn的(氢)氧化物在木质素腐殖化作用中的催化机理,试验共设3个系列处理:针铁矿(Goethite)用G表示,三羟铝石(Bayerite)用B表示,δ-MnO₂用Md表示。复合菌株悬液的接种体积按300 mL培养液接种20 mL进行,接种后,塞好棉塞,用报纸包扎好,在28 ℃恒温条件下摇瓶(180~200 r·min⁻¹)培养110 d,期间按10、30、60、110 d动态取样,分别用G-10、G-30、G-60、G-110、B-10、B-30、B-60、B-110和Md-10、Md-30、Md-60、Md-110表示,取样后立即离心(12 000 r·min⁻¹,10 min),收集含有氧化物的沉淀物质。另外同时设置2个培养110 d后的对照处理,用G-110-CK2、B-110-CK2和Md-110-CK2表示不接种复合菌株悬液,仅在木质素培养液中添加针铁矿、三羟铝石或δ-MnO₂的情况;用G-110-CK3、B-110-CK3和Md-110-CK3表示在缺失木质素,添加针铁矿、三羟铝石或δ-MnO₂的培养液中,仅接种复合

菌株悬液的情况,待110 d培养结束后立即离心,收集沉淀物质。将上述沉淀物质放入60 ℃鼓风干燥箱中烘至恒质量、磨细过0.25 mm筛。针铁矿、三羟铝石和δ-MnO₂的原样品用G-sample、B-sample和Md-sample表示。用30%优级纯H₂O₂对上述沉淀物质及氧化物原样品进行淋洗处理,去除氧化物表面的有机成分,再用去离子水多次洗涤,直至洗液中无有机成分,置入60 ℃鼓风干燥箱中烘至恒质量、粉碎过0.25 mm筛,待检。

1.3 分析方法

SEM(Scanning electron microscopy)。采用SS550型扫描电子显微镜(日本岛津仪器公司)对氧化物样品进行表面微观形貌观察,测试条件为15.00 kV,分辨率为6 nm。

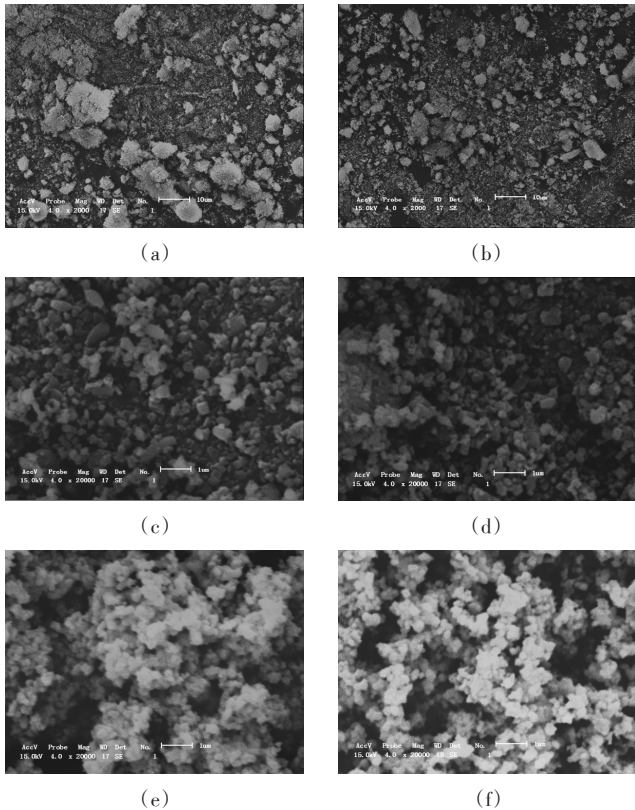
FTIR(Fourier transform infrared spectra)。将氧化物样品与光谱纯KBr 1:100混合、研磨、压片,利用FTIR-850傅立叶变换红外光谱仪(天津港东科技股份有限公司)对样品进行FTIR测试:扫描次数32次,分辨率4 cm⁻¹,Y轴格式为透过率,切趾方式为Triangle,每次采集样品前采集背景并扣除。

XRD(X-ray diffraction)。采用德国bruker粉末X射线衍射仪(D8 FOCUS型)对氧化物样品进行检测,测试条件为CuKα射线,Ni滤波,40 kV,40 mA,LynxEye192位阵列探测器,扫描步长0.01°(2θ),扫描速度每步0.05秒,λ=1.540 598 Å。

2 结果与讨论

2.1 Fe、Al、Mn的(氢)氧化物参与木质素腐殖化作用前后的SEM图像

如图1a所示,针铁矿样品呈绒球状结构,表面有细丝状物质,颗粒大小不一,排列松散,较大颗粒长径约15 μm,参与木质素腐殖化作用后(图1b),形貌特征无明显变化,小颗粒比例增加且颗粒边缘棱角更加分明,大多数颗粒直径小于10 μm,晶体结构中出现大量纳米孔隙,这与结构水的脱除有关。由图1c可见,三羟铝石大多呈多边形颗粒状结构,不规则的晶体排布有着不均匀的尺寸分布,除了结晶相之外,还可以看到具有混合形态的小颗粒,这表明存在无定形或弱结晶的Al(OH)₃,这与Kupecik等^[21]的表述一致。此外,颗粒大小较均匀,直径均在1 μm以下。Tsuchida等^[22]指出,三羟铝石具有近似于六边形最密堆积的羟基晶格结构。而参与木质素转化后(图1d),晶粒轮廓更加清晰,粒径更小,部分颗粒有聚集趋势,晶粒



(a) 针铁矿原样品;(b)针铁矿参与木质素腐殖化作用110 d后的样品;(c)三羟铝石原样品;(d)三羟铝石参与木质素腐殖化作用110 d后的样品;(e)δ-MnO₂原样品;(f)δ-MnO₂参与木质素腐殖化作用110 d后的样品

(a) Original goethite; (b) Goethite after its participation in lignin humification for 110 d; (c) Original bayerite; (d) Bayerite after its participation in lignin humification for 110 d; (e) Original δ-MnO₂; (f) δ-MnO₂ after its participation in lignin humification for 110 d

图1 针铁矿、三羟铝石及δ-MnO₂参与木质素腐殖化作用前后的SEM图像

Figure 1 SEM photographs of goethite, bayerite and δ-MnO₂ before and after their participations in lignin humification

间孔隙增多。由图1e可知,作为一种二维层状结构的纳米金属氧化物,δ-MnO₂为无定型、不规则的球状颗粒,或称类球形粒子,颗粒直径小于0.3 μm,有较强的簇拥或凝聚态势^[23],每一个球状颗粒可视为多孔的微纳米球,或称MnO₂晶胞。参与木质素转化后(图1f),颗粒结合更加松散且空穴增加,微纳米球边缘更加清晰,这与MnO₂表面结合水的脱去有关。

2.2 Fe、Al、Mn的(氢)氧化物参与木质素腐殖化作用的FTIR光谱

如图2a所示,3402~3421 cm⁻¹归属针铁矿H-O-H和O-H的伸缩振动,3130~3163 cm⁻¹为结构OH的伸缩振动,1626~1633 cm⁻¹为水分子的弯曲振动^[24],893 cm⁻¹和795 cm⁻¹归属Fe-OH平面内与平面外的弯

曲振动(δ_{OH} 和 γ_{OH})^[25],638 cm⁻¹为Fe-O的伸缩振动。结合表1,与对照(G-110-CK2和G-110-CK3)相比,针铁矿参与木质素腐殖化作用后可有效降低其表面O-H的伸缩振动,同时增加了水分子的弯曲振动频率。在此过程中,木质素分子及接种的复合菌株通过配体交换过程吸附于针铁矿,来自其羧酸基团的质子与针铁矿表面羟基反应形成水^[26],使得针铁矿表面的结构羟基向水合基转变。与G-10相比,G-30、G-60

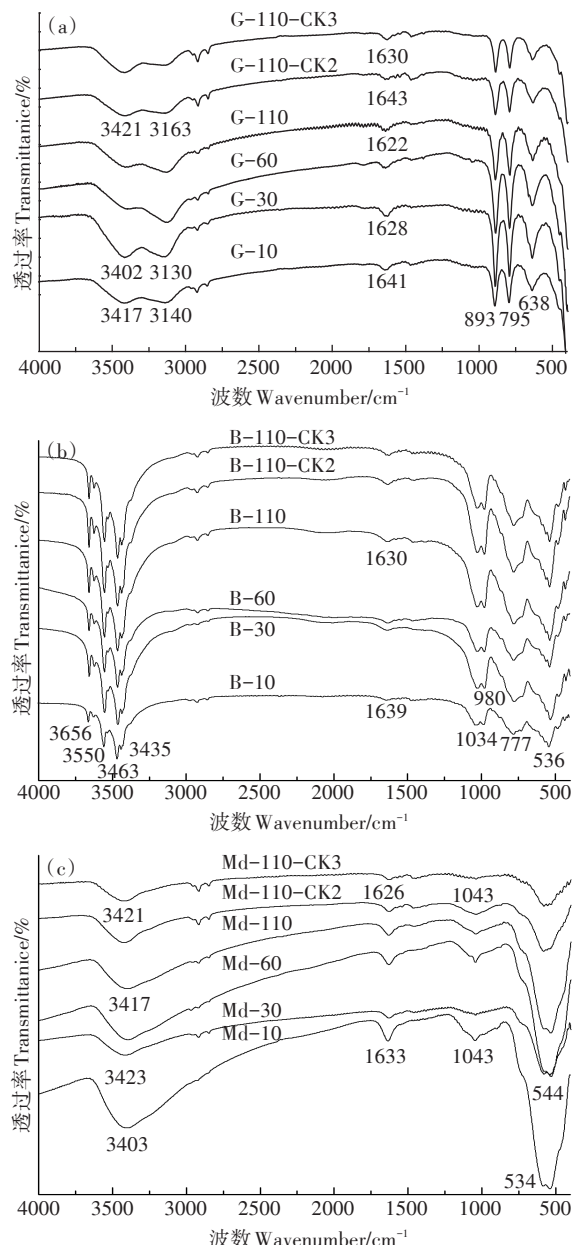


图2 针铁矿、三羟铝石及δ-MnO₂参与木质素腐殖化作用的FTIR光谱

Figure 2 FTIR spectra of goethite, bayerite and δ-MnO₂ involved in lignin humification

和G-110处理的结构OH伸缩振动、水分子弯曲振动、Fe-OH弯曲振动及Fe-O伸缩振动均有不同程度增强。这表明,木质素分子及接种的复合菌株在培养过程中均可与针铁矿表面水合羟基之间形成电荷-偶极键,并以氢键形式结合^[25],使针铁矿表面水合羟基(-OH₂⁺)及结晶水O-H的缔合程度增高。此外,针铁矿通过表面游离羟基与复合菌株以配体交换方式缔结,菌体表面含氧阴离子与针铁矿表面活性基团发生了相互作用,随培养延续,Fe-OH发生质子化,H⁺进入溶液,使Fe-O键有所增强^[26]。可见,配体交换和氢键是针铁矿催化木质素腐殖化作用的主要机制。

如图2b所示,3656、3550、3463 cm⁻¹和3435 cm⁻¹为三羟铝石 α -Al(OH)₃表面OH的伸缩振动,1630~1639 cm⁻¹代表未与Al³⁺配位键合的自由分子水,1043 cm⁻¹和980 cm⁻¹为O-H的弯曲振动,多由Al-OH的振动产生,777、536 cm⁻¹也属三羟铝石的典型吸收峰^[27],分别对应AlO₄四面体中Al-O的不对称伸缩振动以及AlO₆八面体中Al-O的伸缩振动。结合表1可见,与B-10相比,参与木质素转化后的三羟铝石(B-30、B-60和B-110),其表面来自O-H弯曲振动的羟基(Al-OH)能以化学氢键形式与微生物转化的木质素结合,

增加了水合基的振动频率,同时部分OH基团被来自微生物及其转化木质素的羧基所取代,弱化了Al-O键^[28],即降低了AlO₄四面体和AlO₆八面体中的Al-O伸缩振动。可见三羟铝石Al-OH和Al-O键参与了木质素的腐殖化作用,水分子桥键及螯合物的形成使Al-OH₂⁺的振动频率增强^[29]。

由图2c可知,3403~3423 cm⁻¹为 δ -MnO₂表面-OH的伸缩振动,1626~1633 cm⁻¹归属结晶水H-O-H的弯曲振动,1043 cm⁻¹归属Mn-OH的振动,534~544 cm⁻¹为MnO₂中Mn-O的弯曲振动^[23]。结合表1可知,与对照(Md-110-CK2和Md-110-CK3)相比,参与木质素微生物转化的 δ -MnO₂表面吸附水的O-H振动频率有所减弱,说明经微生物转化的木质素分子与 δ -MnO₂表面羟基发生了缔合,形成了外圈配合物^[30]。与Md-10相比,Md-30、Md-60和Md-110处理下的 δ -MnO₂表面结晶水数量减少,相反增加了O-Mn-O键的振动频率,结晶水的减少可以用锰氧化物吸附天然有机质的疏水作用来解释^[31],而Md-10处理下 δ -MnO₂结构中Mn-OH键的振动频率最为强烈,而后因MnO₂表面O-H与微生物转化木质素的含氧阴离子缔结,使得去质子化趋势明显,从而破坏了MnO₂表面

表1 针铁矿、三羟铝石和 δ -MnO₂参与木质素腐殖化作用FTIR光谱主要吸收峰的相对强度(半定量)

Table 1 Main absorption peaks' relative intensities from FTIR spectra of goethite, bayerite and δ -MnO₂ during their participations in lignin humification(semi-quantitative)

针铁矿 Goethite	3401~3423 cm ⁻¹	3133~3143 cm ⁻¹	1626~1644 cm ⁻¹	891~894 cm ⁻¹	795~798 cm ⁻¹	636~641 cm ⁻¹
G-10	21.1	18.1	12.0	6.5	6.8	11.6
G-30	22.6	19.8	12.6	7.1	6.8	12.3
G-60	20.8	19.0	13.0	8.9	7.2	12.1
G-110	21.9	21.6	13.5	7.1	7.0	11.7
G-110-CK2	23.1	20.0	7.6	8.7	6.8	13.3
G-110-CK3	23.8	20.5	9.9	8.4	6.6	11.8
三羟铝石 Bayerite	3435~3656 cm ⁻¹	1628~1639 cm ⁻¹	978~1028 cm ⁻¹	777~781 cm ⁻¹	534~538 cm ⁻¹	—
B-10	40.3	9.8	13.7	10.2	9.2	—
B-30	41.5	12.0	13.4	8.3	7.2	—
B-60	43.4	11.6	13.0	8.8	8.8	—
B-110	41.6	12.8	13.1	7.6	6.5	—
B-110-CK2	39.0	12.8	13.6	7.8	6.9	—
B-110-CK3	41.3	11.8	13.2	9.3	7.9	—
δ -MnO ₂	3402~3423 cm ⁻¹	1626~1633 cm ⁻¹	1043~1047 cm ⁻¹	534~544 cm ⁻¹	—	—
Md-10	29.8	16.5	24.8	17.7	—	—
Md-30	30.7	10.7	19.7	19.8	—	—
Md-60	27.7	12.5	22.9	18.9	—	—
Md-110	30.4	11.6	20.1	18.7	—	—
Md-110-CK2	30.9	12.0	20.6	19.3	—	—
Md-110-CK3	31.9	12.5	17.5	19.6	—	—

OH结构,使Mn-OH中的O-H解离生成Mn-O而使1043~1047 cm⁻¹处吸收峰强度减弱,同时增强了534~544 cm⁻¹处吸收峰的强度^[26]。

2.3 Fe、Al、Mn的(氢)氧化物参与木质素腐殖化作用的XRD谱图

如图3a和表2所示,2θ在21.2°、33.3°、36.7°、53.2°和59.1°处均为针铁矿的特征衍射峰(JCPDS 74-2195),峰形较窄,说明针铁矿样品结晶度较高且在参与木质素转化后,其单体结晶度仍处于良好状态。此外,2θ在这5处特征衍射峰下的d值(晶面间距)分别处于4.14~4.19、2.68~2.69、2.44~2.45、1.71~1.72 nm和1.56 nm,可推断,针铁矿在参与木质素腐殖化作用前后衍射角2θ和晶面间距d仅发生了较小偏移,并未发生物相转变。

如图3b,三羟铝石XRD谱图与Wei等^[27]的报道相似,对应Al(OH)₃(JCPDS Card No. 12-0457),2θ在27.9°、38.2°和64.5°的位置出现了分别对应立方结构勃姆石[γ-AlOOH]的(120)、(140)以及(231)晶面的衍射峰,同时也在2θ为18.9°和20.4°位置上出现了分别对应拜耳石[α-Al(OH)₃]的(001)和(110)晶面的(最强、次强)衍射峰。结合表2可知,仅在培养110 d收集的三羟铝石(B-110)2θ在19.0°、20.6°、28.0°、38.4°和64.5°的峰位向高波方向偏移了0.1°~0.2°,其他处理下的晶面衍射峰位和晶面间距均未发生明显改变,表明三羟铝石参与微生物转化木质素后也未发生物相变化。

由图3c和表2可知,δ-MnO₂在2θ为13.2°、36.6°和65.2°三处存在明显衍射峰,且均为典型δ-MnO₂的衍射峰,对应δ-MnO₂(JCPDS 80-1098)的(001)、(-111)和(-321)晶面^[23]。而在参与木质素转化后,δ-MnO₂系列样品的衍射峰分别在12.0~12.6°、36.6~37.4°和65.8~66.5°出现,衍射峰明显宽化,表明δ-MnO₂的晶型结构不完整,结晶度不高。与δ-MnO₂原样品相比,参与转化的δ-MnO₂仅在低波处衍射峰位发生了改变,由13.2°降至12.0°~12.6°,其他衍射角2θ和晶面间距d均未发生明显变化。

3 结论

(1)针铁矿参与木质素腐殖化作用后,形貌特征无明显变化,晶体结构中出现的纳米孔隙与结构水的脱除有关,其表面水合羟基可与微生物及其转化的木质素间形成电荷-偶极键,使表面水合羟基(-OH₂⁺)及结晶水O-H的缔合程度增强。随培养进行,Fe-OH

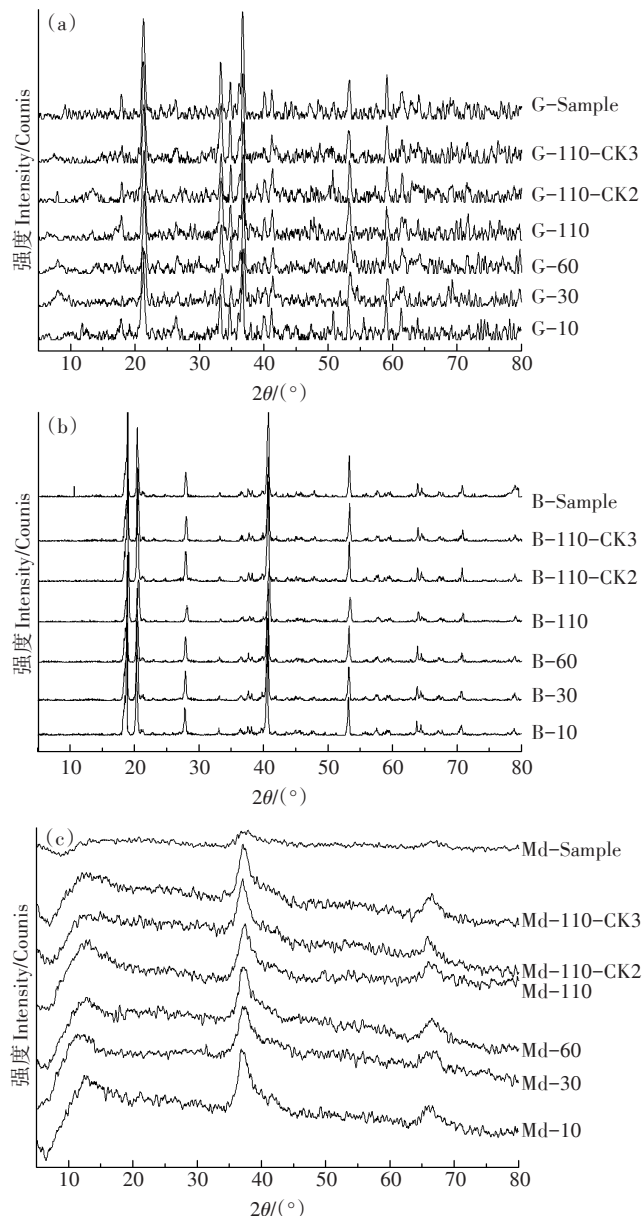


图3 针铁矿、三羟铝石和δ-MnO₂参与木质素腐殖化作用的XRD谱图

Figure 3 XRD spectra of goethite, bayerite and δ-MnO₂ involved in lignin humification

发生质子化,使Fe-O的振动频率有所增强,配体交换和氢键作用在此起主导作用。

(2)三羟铝石参与木质素腐殖化作用后,晶粒轮廓更加清晰,部分颗粒有聚集趋势,其表面Al-OH能以氢键形式与微生物及其转化的木质素结合,增加了水合基的振动频率,同时部分OH基团还可被微生物及其转化木质素的羧基所取代,弱化了Al-O键,降低了AlO₄四面体和AlO₆八面体中Al-O的伸缩振动,水桥键及螯合物的形成使Al-OH₂⁺的振动频率增强。

表2 针铁矿、三羟铝石和 δ -MnO₂参与木质素转化过程XRD特征衍射峰的晶面间距Table 2 Interplanar spacing of XRD spectra diffraction peaks of goethite, bayerite and δ -MnO₂ involved in lignin transformation

处理 Treatments	2θ/(°)					晶面间距 Interplanar spacing/nm																
	G-10	G-30	G-60	G-110	G-110-CK2	G-110-CK3	G-Sample	B-10	B-30	B-60	B-110	B-110-CK2	B-110-CK3	B-Sample	Md-10	Md-30	Md-60	Md-110	Md-110-CK2	Md-110-CK3	Md-Sample	
	21.2	33.3	36.7	53.2	59.1	4.18	2.69	2.45	1.72	1.56												
	21.4	33.3	36.8	53.4	59.2	4.14	2.69	2.44	1.71	1.56												
	21.4	33.3	36.7	53.4	59.0	4.16	2.69	2.45	1.71	1.56												
	21.4	33.3	36.8	53.3	59.0	4.16	2.69	2.44	1.72	1.56												
	21.4	33.4	36.8	53.4	59.2	4.15	2.68	2.44	1.72	1.56												
	21.2	33.3	36.7	53.2	59.1	4.19	2.69	2.45	1.72	1.56												
	21.3	33.3	36.6	53.3	59.0	4.17	2.69	2.45	1.72	1.56												
	18.8	20.3	27.9	38.2	64.4	4.71	4.37	3.20	2.36	1.44												
	18.9	20.4	27.9	38.2	64.4	4.70	4.35	3.19	2.35	1.45												
	18.8	20.3	27.9	38.2	64.4	4.72	4.37	3.19	2.35	1.45												
	19.0	20.6	28.0	38.4	64.5	4.66	4.32	3.18	2.34	1.44												
	18.9	20.4	27.9	38.2	64.5	4.70	4.36	3.19	2.35	1.44												
	18.9	20.4	28.0	38.3	64.9	4.69	4.34	3.18	2.35	1.44												
	18.9	20.4	27.9	38.2	64.5	4.70	4.35	3.19	2.35	1.44												
	12.5	36.7	66.0	—	—	7.10	2.44	1.41	—	—												
	12.0	37.2	66.1	—	—	7.27	2.41	1.41	—	—												
	12.8	37.2	66.5	—	—	6.96	2.41	1.40	—	—												
	12.6	37.4	66.3	—	—	7.02	2.40	1.41	—	—												
	12.2	37.0	65.8	—	—	7.26	2.43	1.42	—	—												
	12.5	37.4	66.3	—	—	7.02	2.40	1.41	—	—												
	13.2	36.6	65.2	—	—	6.70	2.45	1.43	—	—												

(3) δ -MnO₂通过疏水作用参与木质素微生物转化后,颗粒结合更加松散且空穴数量增加,微纳米球边缘锐化,表面结晶水有脱除趋势,相应增加了O-Mn-O键的振动频率,此外,Mn-OH的去质子化也使该趋势更加明显。

(4) Fe、Al、Mn的(氢)氧化物均是通过表面羟基与金属含氧基团来催化木质素的腐殖化作用,其本身并未发生物相改变。

参考文献:

- [1] Kamimura N, Takahashi K, Mori K, et al. Bacterial catabolism of lignin-derived aromatics: New findings in a recent decade[J]. *Environmental Microbiology Reports*, 2017, 9(6):679–705.
- [2] Gonzalo G D, Colpa D I, Habib M H M, et al. Bacterial enzymes involved in lignin degradation[J]. *Journal of Biotechnology*, 2016, 236: 110–119.
- [3] Tuomela M, Oivanen P, Hatakka A. Degradation of synthetic ¹⁴C-lignin by various white-rot fungi in soil[J]. *Soil Biology & Biochemistry*, 2002, 34(11):1613–1620.
- [4] Zhang Z C, Zhao Y, Wang R X, et al. Effect of the addition of exogenous precursors on humic substance formation during composting[J]. *Waste Management*, 2018, 79:462–471.
- [5] Mapelli F, Marasco R, Ballo A, et al. Mineral–microbe interactions: Biotechnological potential of biowathering[J]. *Journal of Biotechnology*, 2012, 157(4):473–481.
- [6] Hayes M H B, Swift R S. An appreciation of the contribution of Frank Stevenson to the advancement of studies of soil organic matter and humic substances[J]. *Journal of Soils and Sediments*, 2018, 18 (4) : 1212–1231.
- [7] Tan K H. Humic matter in soil and the environment: Principles and controversies[M]. 2th Edition. New York: CRC Press, 2014:333–393.
- [8] Fukuchi S, Miura A, Okabe R, et al. Spectroscopic investigations of humic-like acids formed via polycondensation reactions between glycine, catechol and glucose in the presence of natural zeolites[J]. *Journal of Molecular Structure*, 2010, 982:181–186.
- [9] Kaiser M, Zederer D P, Ellerbroek R H, et al. Effects of mineral characteristics on content, composition, and stability of organic matter fractions separated from seven forest topsoils of different pedogenesis[J]. *Geoderma*, 2016, 263:1–7.
- [10] Sarkar B, Singh M, Mandal S, et al. Clay minerals–organic matter interactions in relation to carbon stabilization in soils[J]. *The Future of Soil Carbon*, 2018; 71–86.
- [11] Poggenburg C, Mikutta R, Schippers A, et al. Impact of natural organic matter coatings on the microbial reduction of iron oxides[J]. *Geochimica et Cosmochimica Acta*, 2018, 224:223–248.
- [12] Herndon E, AlBashaireh A, Singer D, et al. Influence of iron redox cycling on organo–mineral associations in Arctic tundra soil[J]. *Geochimica et Cosmochimica Acta*, 2017, 207:210–231.

- [13] Schneider M P W, Scheel T, Mikutta R, et al. Sorptive stabilization of organic matter by amorphous Al hydroxide[J]. *Geochimica et Cosmochimica Acta*, 2010, 74:1606–1619.
- [14] Miltner A, Zech W. Beech leaf litter lignin degradation and transformation as influenced by mineral phases[J]. *Organic Geochemistry*, 1998, 28:457–463.
- [15] Li H, Lee L S, Schulze D G, et al. Role of soil manganese in the oxidation of aromatic amines[J]. *Environmental Science & Technology*, 2003, 37:2686–2693.
- [16] Shindo H, Huang P M. Catalytic effect of manganese (IV), iron (III), aluminum, and silicon oxides on the formation of phenolic polymers [J]. *Soil Science Society of America Journal*, 1984, 48(4):927–934.
- [17] Chen Y M, Tsao T M, Liu C C, et al. Polymerization of catechin catalyzed by Mn–Fe and Al–oxides[J]. *Colloids and Surfaces B: Biointerfaces*, 2010, 81(1):217–223.
- [18] Wang M C, Huang P M. Ring cleavage and oxidative transformation of pyrogallol catalyzed by Mn, Fe, Al, and Si oxides[J]. *Soil Science*, 2000, 165(12):934–942.
- [19] Wu J Q, Qi H S, Huang X N, et al. How does manganese dioxide affect humus formation during biocomposting of chicken manure and corn straw[J]. *Bioresource Technology*, 2018, 269:169–178.
- [20] Yuan Y, He X S, Xi B D, et al. Polarity and molecular weight of com- post-derived humic acid affect Fe (III) oxides reduction[J]. *Chemosphere*, 2018, 208:77–83.
- [21] Kupcik T, Rabung T, Lützenkirchen J, et al. Macroscopic and spectroscopic investigations on Eu (III) and Cm (III) sorption onto bayerite (β -Al(OH)₃) and corundum (α -Al₂O₃)[J]. *Journal of Colloid and Interface Science*, 2016, 461:215–224.
- [22] Tsuchida T, Norio Ichikawa. Mechanochemical phenomena of gibbsite, bayerite and boehmite by grinding[J]. *Reactivity of Solids*, 1989, 7:207–217.
- [23] Huang Y J, Lin Y L, Li W S. Controllable syntheses of α - and δ -MnO₂ as cathode catalysts for zinc-air battery[J]. *Electrochimica Acta*, 2013, 99:161–165.
- [24] Ruan H D, Frost R L, Klopogge J T. The behavior of hydroxyl units of synthetic goethite and its dehydroxylated product hematite[J]. *Spectrochimica Acta Part A*, 2001, 57:2575–2586.
- [25] Rong X M, Chen W L, Huang Q Y, et al. The adhesion amount of *Salmonella typhimurium* to quartz, albite, feldspar, and magnetite was correlated positively with the hydrophobicity and positive charge of the cells[J]. *Colloids and Surfaces B: Biointerfaces*, 2010, 80:79–85.
- [26] Parfitt R L, Fraser A R, Farmer V C. Adsorption on hydrous oxides. III. Fulvic acid and humic acid on goethite, gibbsite and imogolite[J]. *Journal of Soil Science*, 1977, 28:289–296.
- [27] Wei G Y, Qu J K, Zheng Y D, et al. Crystallization behaviors of bayerite from sodium chromate alkali solutions[J]. *Transactions of Nonferrous Metals Society of China*, 2014, 24:3356–3365.
- [28] Stevenson F J, Vance G F. The environmental chemistry of aluminum [M]. Boca Raton: CRC Press, 1989:117–145.
- [29] Tombacz E, Dobos A, Szekeres M, et al. Effect of pH and ionic strength on the interaction of humic acid with aluminium oxide[J]. *Colloid and Polymer Science*, 2000, 278(4):337–345.
- [30] Gulley-Stahl H, Hogan P A, Schmidt W L, et al. Surface complexation of catechol to metal oxides: An ATR-FTIR, adsorption, and dissolution study[J]. *Environmental Science & Technology*, 2010, 44 (11):4116–4121.
- [31] Allard S, Gutierrez L, Fontaine C, et al. Organic matter interactions with natural manganese oxide and synthetic birnessite[J]. *Science of the Total Environment*, 2017, 583:487–495.